Molecular Structure of Phthalocyaninatotin(II) Studied by Gas-Phase Electron Diffraction and High-Level Quantum Chemical Calculations

Tatyana Strenalyuk, Svein Samdal,* and Hans Vidar Volden

Center for Theoretical and Computational Chemistry (CTCC), Department of Chemistry, University of Oslo, P.O. Box 1033 Blindern, NO-0315 Oslo, Norway

Received: May 31, 2008; Revised Manuscript Received: June 27, 2008

The molecular structure of phthalocyaninatotin(II), Sn(II)Pc, is determined by density functional theory (DFT/B3LYP) calculations using various basis sets and gas-phase electron diffraction (GED). The quantum chemical calculations show that Sn(II)Pc has C_{4v} symmetry, and this symmetry is consistent with the structure obtained by GED at 427 °C. GED locates the Sn atom at $h(\mathrm{Sn}) = 112.8(48)$ pm above the plane defined by the four isoindole N atoms, and a N−Sn bond length of 226.0(10) pm is obtained. Calculation at the B3LYP/cc-pVTZ/cc-pVTZ-PP(Sn) level of theory gives $h(\mathrm{Sn}) = 114.2$ pm and a N−Sn bond length of 229.4 pm. The phthalocyanine (*Pc*) macrocycle has a slightly nonplanar structure. Generally, the GED results are in good agreement with the X-ray structures and with the computed structure; however, the comparability between these three methods has been questioned. The N−Sn bond lengths determined by GED and X-ray are significantly shorter than those from the B3LYP predictions. Similar trends have been found for C−Sn bonds for conjugated organometallic tin compounds. Computed vibrational frequencies give five low frequencies in the range of 18−54 cm^{-1}, which indicates a flexible molecule.

Introduction

Tinphthalocyanine (SnPc) chemistry has gained considerable attention due to commercial applications such as organic semiconductors,[1] organic materials for nonlinear optical devices,[2,3] precursors for a new class of electrically conductive polymers,[4] precursors for organic thin films of various properties,[5] and as corrosion inhibitors.[6] The protruding central atom makes the SnPc derivatives interesting for a possible application as a single-molecular storage device.[7]

The thermal and chemical stability of the phthalocyanine complexes makes them suitable for structural researches. Despite the large number of publications on properties and crystal structures of phthalocyanine complexes, only a few papers deal with phthalocyaninatotin(II) (Sn(II)Pc). The same applies to tin porphyrin (Sn(II)P), where Sn(II) has an uncommon oxidation state with a strong tendency for oxidation to Sn(IV).[8] The ionic radius of four-coordinated Sn(II)[9] is 93 pm, which is too large to be accommodated into the porphyrin inner cavity of radius[10] 196−206 pm. Absorption spectra and NMR data confirm that the Sn(II) atom is above the porphyrin plane.[11] However, Sn(IV) (with coordination number 4) has an ionic radius[9] of 69−71 pm, and this ionic radius is small enough for Sn(IV) to be within the porphyrin plane ($\mathrm{Sn(IV)PCl_2}$). The Sn(IV) is smaller than the Zn atom of radius[9] 74 pm, and it was found by GED and quantum chemical calculations that Zn is in the center of planar phthalocyaninatozinc(II), $\mathrm{C_{32}H_{16}N_8Zn}$,[12] and perfluorinated phthalocyaninatozinc(II), $\mathrm{C_{32}F_{16}N_8Zn}$.[12]

A comparison of typical structures of phthalocyanine complexes with typical porphyrin structures shows that the distances between opposite isoindole N atoms in phthalocyanine complexes (380−400 pm) are shorter than the corresponding distances in porphyrins (about 410 pm).[13] Therefore, Sn(II) is expected to be out of the phthalocyanine plane.

The most probable molecular symmetry of Sn(II)Pc is C_{4v}, which is close to the experimental X-ray crystal structures. The first X-ray and Mössbauer studies of triclinic Sn(II)Pc published in 1970[14] have shown that the Sn atom is located 111 pm above the plane that is composed by the four isoindole N atoms. The Sn atom is forced out of the macrocycle because the Sn(II) atom diameter is about 50 pm larger than the maximum size suitable for the Pc inner cavity. The four N−Sn bonds with an average length of 225.3(10) pm and a lone pair form a square-pyramidal arrangement about the Sn atom. The Pc ligand described as "saucer-shaped"[14] is composed by four essentially planar isoindole subunits where the outer C atoms deviate slightly from the inner plane.

A recent X-ray analysis of triclinic Sn(II)Pc[15] finds the Sn atom 112.9 pm above the plane of the four isoindole N atoms, and the N−Sn bond lengths vary from 226.0(7) to 227.3(5) pm. These numbers are in good agreement with the previous X-ray[14] results, and the N−Sn bond lengths are shorter than the average N−Sn bond lengths of 234.7(7)[16] and 231.9(3)[17] pm found for the γ- and the β-forms of diphthalocyaninatotin(IV), $\mathrm{Sn(IV)Pc_2}$. The two phthalocyanine ring systems of the γ- and the β-forms are rotated 42[16] and 38°[17] with respect to each another (eclipsed conformation 0°) and form sandwich-type complexes with a square antiprismatic coordination about the Sn(IV) atom. The N−Sn bond length in the chloro(trimethyl)pyridinetin(IV) is 226.1 pm, but the Sn atom is, in this case, surrounded by five atoms in a trigonal-bipyramidal configuration.[18]

There are few articles available on quantum chemical calculations on Sn(II)Pc. DFT(LDA)/DZP calculations[19] lead to a stationary point close to the expected C_{4v} symmetry. RHF/SBK(d) calculations[19] give a low-symmetry structure, and this result is obviously due to neglect of electron correlation in the single determinant HF method. B3LYP/LANL2DZ calculations[20] have been used to optimize the geometry for several phthalocyanine complexes, among them SnPc, and for calculation of vibrational frequencies.

* To whom correspondence should be addressed. E-mail: svein.samdal@kjemi.uio.no. Tel: +47 2285 5458. Fax: +47 2285 5441.

10.1021/jp804809e CCC: $40.75
Published on Web 09/04/2008

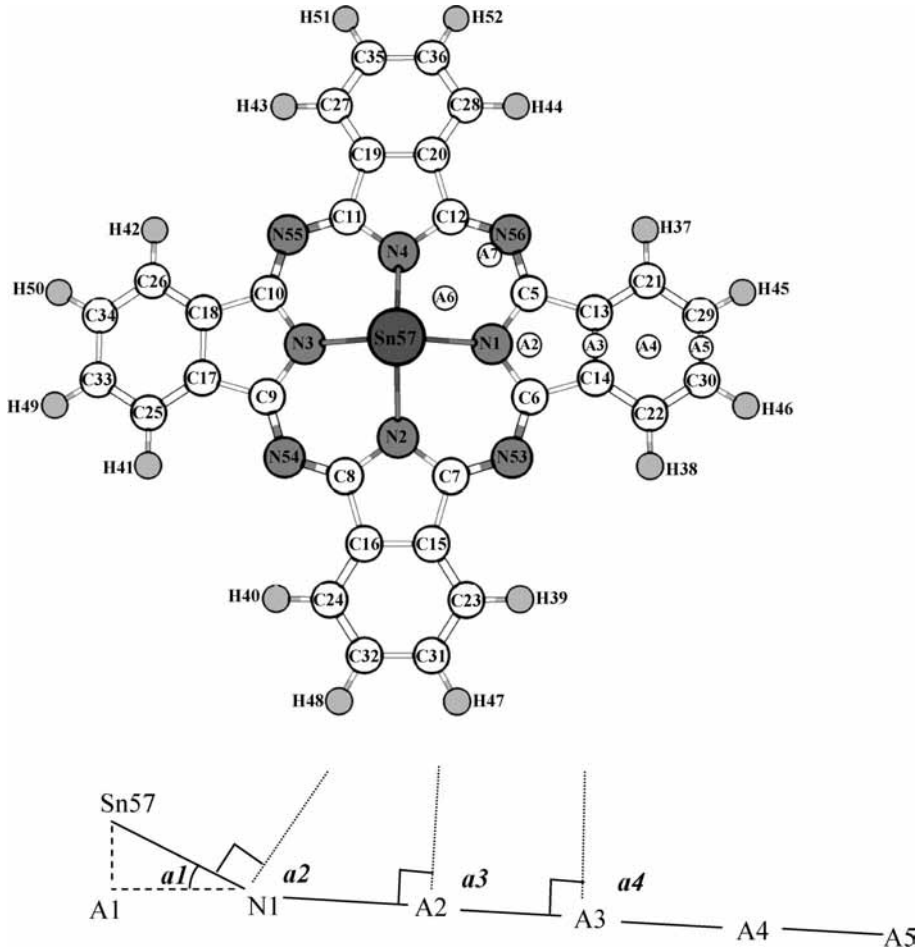

Figure 1. Molecular view of Sn(II)Pc and atom numbering together with some auxiliary points A1−A7 used to describe the molecular geometry. The figure below shows the possible bending of the isoindole unit under C_{4v} symmetry.

Only one article in the available literature on various SnPc's concerns the experimental molecular structure of Sn(II)Pc in gas phase,[21] and this GED investigation confirms the nonplanar C_{4v} geometry where the Sn atom is 101(10) pm above the Pc plane. The nonplanarity of the Pc macrocycle has been modeled by rotation of the planar isoindole units about the C−N bonds (C5−N56 and C6−N53) in such a way that the four atoms N53, C6, C5, and N56 are in one plane (see Figure 1). The N−Sn bond length[21] was found to be 220.1 pm, which is about 6.5 pm shorter than that found by X-ray.[15] Some of the C−C bond lengths and the C−C−C and N−C−N angles are in considerable disagreement with the X-ray structures.

Due to the apparent disagreement between the published GED structure[21] and the X-ray structures, low accuracy and precision of the GED results, and our recent successful studies[12,22] on similar molecules where we have demonstrated the validity of the GED method for the accurate structure determination of Pc complexes in the gas phase, we wanted to reinvestigate Sn(II)Pc. In this work, on the basis of a much larger data sample and supported with high-level quantum chemical calculations and inclusion of vibrational corrections, a much higher accuracy and precision and more details about its geometry are expected. In this paper, we present our results on Sn(II)Pc with the formula $C_{32}H_{16}N_8Sn$, systematic name [29H,31H-phthalocyaninato-(2-)-κN29, κN30, κN31, κN32]tin(II), and trivial name phthalocyaninatotin(II) (Sn(II)Pc).

Experimental Section

Sn(II)Pc was obtained from Aldrich and used without further purification.

TABLE 1: Experimental Conditions for Sn(II)Pc

nozzle-to-plate distance/mm	498.63	249.06
electron wavelength/pm	5.82	5.82
nozzle temperature/°C	427	427
s ranges/nm^{-1}:		
x-direction	21.25−148.75	41.25−300.00
y-direction	20.00−132.50	40.00−262.50
Δs/nm^{-1}	1.25	1.25
number of plates	4	4
degree of polynomial[a]	8	10

[a] Degree of polynomial used in the background subtraction.

The GED data were recorded on the Balzers KD-G2 unit[23] at the University of Oslo. The experimental conditions are collected in Table 1. More details about handling[24] of the experimental data and their processing[25] are given elsewhere. A brief description of the GED method particularly relevant for this investigation is given in ref 22.

Quantum Chemical Calculations. The present calculations on Sn(II)Pc were performed using the Gaussian03[26] program package running on the HP "superdome" facilities in Oslo.

The molecular view of Sn(II)Pc and the numbering of the atoms are shown in Figure 1. The following models were tested:

(1) C_{4v}, where the four isoindole subunits are equivalent and the Sn atom is out of the "saucer-shaped"[14] Pc macrocycle.

(2) C_{4v}, where the Sn atom is above a planar Pc macrocycle.

(3) C_{2v}, which possesses two nonequivalent pairs of the isoindole subunits. Vertical mirror planes go through the Sn atom and the opposite isoindole N atoms.

TABLE 2: Calculated Structural Parameters for Sn(II)Pc[a]

	DZVP			LANL2DZdp		6−311++G**/cc-pVTZ-PP	cc-pVTZ/cc-pVTZ-PP
parameter	C_{4v}[e]	C_{4v}[f]	D_{2h}	C_{4v}[e]	C_{4v}[f]	C_{4v}[e]	C_{4v}[e]
			Bond Lengths/pm				
h(Sn)	115.4[b]	114.2[b]	0.0/0.0[d]	110.0[b]	108.6[b]	114.4[b]	114.2[b]
N1···N3	398.8	397.4	409.5/407.4[c]	397.3	396.2	398.6	398.0
N1−Sn57	230.4	229.1	204.8/203.7[c]	227.1	225.9	229.8	229.4
N1−C5	137.6	137.7	140.5/142.6[c]	137.9	138.0	137.2	136.9
C5−N56	133.1	133.3	136.7/129.4[c]	133.3	133.4	132.7	132.4
C5−C13	146.1	146.1	141.3/146.7[c]	146.3	146.3	145.9	145.5
C13−C14	141.0	141.1	143.9/141.0[c]	141.2	141.3	140.7	140.3
C13−C21	139.9	139.9	141.9/139.7[c]	140.2	140.2	139.4	139.0
C21−C29	139.7	139.7	137.9/139.9[c]	139.9	140.0	139.2	138.8
C29−C30	141.2	141.2	143.2/140.8[c]	141.6	141.6	140.7	140.2
C21−H37	108.6	108.7	108.6/108.6[c]	108.9	108.9	108.3	108.1
C29−H45	108.7	108.8	108.7/1.08.7[c]	109.0	109.0	108.4	108.2
			Bond Angles/degrees				
C5−N1−Sn57	123.2	120.2	124.6/124.5[c]	123.3	120.7	123.3	123.3
C5−N1−C6	108.9	109.1	110.7/111.0[c]	108.6	108.8	109.1	109.1
C5−N56−C12	123.8	124.0	126.4	123.5	123.6	124.1	124.2
N1−C5−C13	109.0	108.9	106.7/105.8[c]	109.2	109.1	109.0	108.9
N1−C5−N56	127.8	127.6	126.6/127.8[c]	127.8	127.6	127.8	127.8
C5−C13−C14	106.5	106.5	108.0/108.7[c]	106.5	106.5	106.5	106.5
C14−C13−C21	121.2	121.1	120.3/121.0[c]	121.2	121.2	121.1	121.1
C13−C21−C29	117.7	117.7	118.3/118.0[c]	117.6	117.6	117.7	117.7
C21−C29−C30	121.2	121.2	121.4/121.0[c]	121.2	121.2	121.2	121.2
C13−C21−H37	120.8	120.7	120.1/120.5[c]	120.8	120.8	120.7	120.7
C21−C29−H45	119.7	119.7	119.7/119.6[c]	119.7	119.7	119.6	119.6
			Bending Angles/degrees				
a1[g]	30.1	29.9	0.0/0.0[c]	29.0	28.7	29.9	29.9
a2[g]	70.3	60.1	90.0/90.0[c]	70.3	61.3	71.0	71.0
a3[g]	91.8	90.0	90.0/90.0[c]	91.8	90.0	91.9	92.0
a4[g]	91.4	90.0	90.0/90.0[c]	91.1	90.0	91.4	91.5
A6−A7−N56[g]	175.4	180.0	180.0	175.8	180.0	175.3	175.2
N56−A7−A6−Sn57	0.0	0.0	0.0	0.0	0.0	0.0	0.0

[a] All quantum chemical calculations were performed using B3LYP. [b] *h*(Sn) = Sn57−A1; see Figure 1. [c] There are two nonequivalent isoindole subunits. The first value is a structural parameter associated with isoindole subunit involving N1 or N3, and the last value is a parameter associated with isoindole subunit involving N2 or N4 atoms. [d] The first value is the distance of the Sn atom to the plane containing N1 and N3, and the last value is the distance to the plane containing N2 and N4. [e] The Sn atom is above the inner cavity of the nonplanar macrocycle. [f] The Sn atom is above the central cavity of a planar Pc macrocycle. [g] See text and Figure 1 for more details.

(4) D_{2h}, where the Sn atom is placed into the central cavity and is bonded to two pairs of equivalent isoindole subunits.

(5) D_{4h}; the Sn atom is located in the cavity of a planar Pc ring.

Taking into account the neglect of electron correlation in the Hartree−Fock (HF) theory and the time-consuming perturbation theory methods such as MP2, the density functional theory (DFT) is the most suitable method for the study of large and complex molecular systems such as phthalocyanine complexes.

The calculations were performed at the density functional theory B3LYP[27,28] level using basis sets such as (i) the high-quality double-ζ split-valence polarized basis set, DZVP,[29,30] (ii) the double-ζ polarized basis set with diffuse functions and electron core potential, LANL2DZdp,[31,32] (iii) the Pople's triple-ζ split-valence polarized basis set with diffuse functions, 6-311++G**,[33,34] for H, C, and N and the Dunning's correlation-consistent polarized valence triple-ζ basis set cc-pVTZ-PP[35] including a small-core relativistic pseudopotential to replace 28 core electrons ([Ar] + 3d)[36] for Sn, and (iv) the cc-pVTZ[37] basis set for H, C, and N and the cc-pVTZ-PP[35,36] for Sn.

B3LYP calculations using 6-311++G** and cc-pVTZ basis sets were successful for some previously studied Pc molecules,[12,22] where the calculated structures are in good agreement with the experimental structures. The cc-pVTZ-PP(Sn) basis set on the Sn atom has been tested for small organotin molecules,[38,39] where generally good agreement between calculated and experimental structures was obtained. However, there are indications that the bond lengths to the Sn atom are calculated to be too short.

Force field calculations were performed for all geometries optimized using DZVP and LANL2DZdp basis sets in order to ensure that the obtained structures correspond to minima on the potential energy surface. The force field, calculated at B3LYP/6-311++G**/cc-pVTZ-PP(Sn) theory level, was used in the SHRINK program[40,41] to obtain vibrational correction terms.

The time-consuming calculations with the large basis sets (iii) and (iv) were mainly performed under C_{4v} symmetry and without calculation of the molecular force field.

The calculated geometrical parameters and corresponding energies together with energy differences between tested models are summarized in Tables 2 and 3, respectively.

Structural Analysis. ***Models and Constraints.*** The molecular view and the numbering of the atoms are shown in Figure 1. The C_{4v} symmetry model was chosen as a starting point for the structural analysis.

The Pc macrocycle was modeled by 90° rotations of the isoindole subunit (N1, C5, C6, C13, C14, C21, C22, C29, C30, H37, H38, H45, and H46) and the attached N56 bridged atom about four-fold symmetry axis passing through the Sn atom. A

TABLE 3: Calculated Energies of Sn(II)Pc

	C_{4v}[c]	C_{4v}[d]	D_{2h}[e]
B3LYP/DZVP			
E[a]	−7692.086506	−7692.081069	−7691.990016
ΔE[b]	0.0	14.3	253.3
$E + E_0$[a]	−7691.674477	−7691.669201	−7691.580353
$\Delta(E + E_0)$[b]	0.0	13.9	247.1
B3LYP/LANL2DZdp			
E[a]	−1670.757261	−1670.752660	
ΔE[b]	0.0	12.1	
$E + E_0$[a]	−1670.346042	−1670.34.1346	
$\Delta(E + E_0)$[b]	0.0	12.3	
B3LYP/6-311++G**/cc-pVTZ-PP			
E[a]	−1881.967647		
$E + E_0$[a]	−1881.557152		
B3LYP/cc-pVTZ/cc-pVTZ-PP			
E[a]	−1882.113225		

[a] These energies are in hartree/molecule. [b] The energy differences are in kJ/mol. [c] The Sn atom is above the inner cavity of the nonplanar macrocycle. [d] The Sn atom is above the inner cavity of the planar Pc macrocycle. [e] The Sn atom is within the central cavity of the macrocycle.

mirror plane through the N1 atom and auxiliary points A3−A5 (see Figure 1) allows a description of the Sn(II)Pc molecular geometry using the following set of independent structural parameters: (bond lengths) N1−C5, C5−N56, C5−C13, C13−C14, C13−C21, C21−C29, C29−C30, C21−H37, and C29−H45; (bond angles) C5−N1−C6, C14−C13−C21, C13−C21−H37, and C21−C29−H45. The benzene ring was assumed to be planar.

The position of the Sn atom is determined by the N1−Sn57 bond length and the a1 = the A1−N1−Sn57 angle (where the A's are auxiliary points here and further in the text; see Figure 1).

The shape of the Pc ligand is modeled by using three bending angles (Figure 1), A2−N1−Sn57 = a2 + 90°, which determines the pyramidality of the N1 atom, N1−A2−A3 = a3 + 90°, which corresponds to the N1−C6−C5-C13 dihedral angle equivalent to the envelope angle of the pyrrole ring, and A2−A3−A4 = a4 + 90°, which corresponds to the C5−C13−C14−C22 dihedral angle defining the folding of the isoindole subunit about the C13−C14 bond. The A6−A7−N56 angle defines the position of the N56 atom with respect to the plane through the atoms N1, C5, C12, and N4 and consequently defines a boat or chair conformation dependent on the N56−A7−A6−Sn57 dihedral angle. The N56−A7−A6−Sn57 dihedral angle gives a boat conformation if it is 0° and a chair conformation if it is 180°. The presence of several low frequencies makes it difficult to accurately determine these bending angles. The B3LYP-computed and least-squares-refined values of a2, a3, a4, and A6−A7−N56 are compared in Table 4.

GED does not allow accurate determination of differences between parameters if the bond type and bond lengths are similar. Due to low scattering power of the H atom, the structural parameters involving the H atoms cannot be refined accurately. Therefore, the following constraints between independent parameters were introduced: C13−C21 = C13−C14 + Δ1, C21−C29 = C13−C14 + Δ2, C29−C30 = C13−C14 + Δ3, C29−H45 = C21−H37 + Δ4, and C5−N56 = N1−C5 + Δ5. The differences, Δ1−Δ5, were taken from the B3LYP/6-311++G**/cc-pVTZ-PP(Sn) optimized geometry, and they are −1.27, −1.52, −0.04, 0.11, and −4.52 pm, respectively. Attempts were made to refine some of these differences. However, only the difference between the N1−C5 and C5−N56 bond lengths was successfully refined and gave better agreement between experimental and theoretically calculated radial distribution curves (Figure 3). The Δ1−Δ4 differences were fixed at their DFT-calculated values.

Vibrational Corrections. The shrinkage effect was included in the analysis by using the SHRINK program,[40,41] which uses the curvilinear treatment of the vibrating atoms. The calculated root-mean-square amplitudes of vibration (u_{h1} values) and the shrinkage corrections (k_{h1} values) were calculated using the B3LYP/6-311++G**/cc-pVTZ-PP(Sn) force field, and the $r_e - r_a$ differences were estimated. The u values were refined in groups referring to the peaks on the radial distribution curve (Figure 3) to which they belong. All refinements were performed by the least-squares fitting program KCED25.[42] The following correlation coefficients had values larger than |0.7|: A2−N1−Sn57/N1−A2−A3 = −0.88, N1−C5/Δ5 = −0.75, C13−C14/ the amplitudes' group corresponding to the first peak on the radial distribution curve (Figure 3) = −0.77.

The final values of structural parameters together with the B3LYP/cc-pVTZ/cc-pVTZ-PP(Sn) predicted counterparts are listed in Table 4. The experimental and theoretical intensities and the radial distribution curves are shown in Figures 2 and 3, respectively.

Results and Discussion

Quantum Chemical Calculations. The most important calculated structural parameters for Sn(II)Pc are listed in Table 2. The energies are listed in Table 3, which shows that the C_{4v} symmetry structure where the Sn atom is out of the center of the nonplanar Pc macrocycle is the most stable form for Sn(II)Pc. It should be noted that the geometry optimized under C_{2v} symmetry converged to the C_{4v} symmetry. This C_{4v} symmetry was also found for tin phorphyrin, Sn(II)P, where the geometry optimizations were performed under C_{4v} and D_{4h} symmetries.[43] The DFT/TDDFT method was used in conjunction with the STO basis of triple-ζ quality plus one polarization function for all atoms and a small core definition for Sn ([Kr]). These calculations on Sn(II)P gave a nonplanar C_{4v} structure, where the Sn atom is 107 pm above the porphyrin plane, and this form is 248 kJ/mol more stable than its planar D_{4h} structure.

The geometry calculations on Sn(II)Pc using B3LYP/DZVP and D_{4h} symmetry did not converge, and a rather strange behavior of the Gaussian03 program was observed. However, reducing the symmetry to D_{2h} removed the difficulties for convergence, and to our surprise, the D_{2h} structure given in Table 2 represents an energy minimum with no imaginary frequencies. The B3LYP/DZVP calculations predict two different stable isomers, and the energy difference between the two isomers is 247 kJ/mol. An inspection of Table 2 shows that the bond lengths obtained for Sn(II)Pc for the D_{2h} isomers are completely different from the corresponding bond lengths for the C_{4v} isomer. The N−Sn bond lengths for the D_{2h} isomer are much shorter than the N−Sn bond lengths for the C_{4v} isomer, whereas the size of the Pc hole is about 10 pm larger for the D_{2h} isomer. It is interesting to notice that the cavity diameter for the D_{2h} isomer N1···N3/N2···N4 = 409.5/407.4 pm is considerably larger than the maximum diameter normally found for phthalocyanine complexes (400 pm).[13] The structural parameters for the D_{2h} isomer are split into two groups due to symmetry. The N1−C5/N2−C7 bond lengths of 140.5/142.6 pm for the D_{2h} isomer are longer than the corresponding N1−C5 bond length of 137.6 pm for the C_{4v} isomer. The C5−N56/C12−N56 bond lengths of 136.7/129.4 pm for the D_{2h} isomer are shorter and longer

TABLE 4: Experimental and Calculated Structural Parameters for Sn(II)Pc[a]

	GED		SHRINK			B3LYP	GED[44]	X-ray	
parameter	$r_{e(ave)}$	u_{exp}	u_{h1}[b]	k_{h1}[b]	$r_e - r_a$	cc-pVTZ/cc-pVTZ-PP	r_a	triclinic[14]	triclinic[15]
					Bond Lengths/pm				
h(Sn)	112.8(48)[c,e]					114.2	101(10)	111.0	112.9
N1−Sn57	226.0(10)	9.6[f]	9.6	0.10	−1.65	229.4	220.1	225.3	226.7
N1−C5	137.5(8)	5.3(3)	5.2	0.23	−0.05	136.9	140.9(31)	137.3	136.9
N56−C5	134.3(7)[d]	4.9(3)	4.7	−0.03	−0.54	132.4		132.8	133.0
C5−C13	146.3(7)	5.5(3)	5.4	−0.05	−0.60	145.5	143.8(47)	145.6	146.0
C13−C14	140.5(6)	5.1(3)	4.9	−0.16	−0.46	140.3	153(10)	139.1	139.7
C13−C21	139.3(6)[d]	5.0(3)	4.9	0.03	−0.46	139.0	139.2(10)[h]	139.5	138.1
C21−C29	139.1(6)[d]	5.0(3)	4.8	0.08	−0.36	138.8		138.6	137.9
C29−C30	140.6(6)[d]	5.1(3)	5.0	0.07	−0.40	140.2		140.0	138.9
C21−H37	111.4(11)	7.6[f]	7.6	0.01	−1.67	108.1	109.9(46)[i]		
C29−H45	111.5(11)[d]	7.6[f]	7.6	0.01	−1.68	108.2			
					Bond Angles/degrees				
C5−N1−Sn57	123.5(7)[e]					123.3			122.8
C5−N1−C6	107.5(5)					109.1	110.5(30)	108.2	108.3
C5−N56−C12	122.5(9)[e]					124.2	124.6	122.4	122.3
N1−C5−C13	110.0(3)[e]					108.9	107.1	109.2	112.2
N1−C5−N56	127.2(4)[e]					127.8	125.5(28)	128.1	128.2
C5−C13−C14	106.1(3)[e]					106.5	106.1	106.6	106.4
C14−C13−C21	121.6(2)					121.1	118.3(21)	121.3	121.1
C13−C21−C29	116.8(4)[e]					117.7	121.9	117.3	117.6
C21−C29−C30	121.6(2)[e]					121.2		121.3	121.3
C13−C21−H37	120.7[f]					120.7	120.1(78)		
C21−C29−H45	119.6[f]					119.6			
					Bending Angles/degrees				
a1	29.7(5)					29.9		∼29.5	
a2	69.2(29)					70.9			
a3	85.6(43)					92.0			
a4	95.0(36)					91.5			
A6−A7−N56	169.8(38)					175.2			
N56−A7−A6−Sn57	0.0[e]					0.0			
R_f, %	3.99[g]								

[a] Parenthesized values are error estimates defined as $2.5(\sigma^2_{lsq} + (0.001 \times r)^2)^{1/2}$ for distances and $2.5\sigma_{lsq}$ for angles and amplitudes, where σ_{lsq} is one standard deviation taken from the least-squares refinements using a diagonal weight matrix, and the $0.001 \times r$ term represents 0.1% uncertainty in the electron wavelength. The errors are in the units of the last digits. [b] Curvilinear treatment of the vibrating atoms. [c] r_a parameter. [d] This value was calculated by using constraints between parameters (see text). [e] Dependent parameter where 0° represents a boat conformation of the six-membered ring consisting of the atoms Sn57, N1, C5, N56, C12, and N4, and 180° represent a chair conformation. [f] These parameters were fixed at their B3LYP/6-311++G**/cc-pVTZ-PP calculated values. [g] $R_f = [\sum_s w(I_s^{obs} - I_s^{calc})^2/\sum_s w(I_s^{obs})^2] * 100\%$, where w is a weight function usually equal to 1 and I is the molecular modified intensity. [h] This value is the average C−C distance for the benzene ring. [i] This is the average C−H bond length.

than the C5−N56 bond length for the C_{4v} isomer, which is 133.1 pm. The bond lengths between atoms for the D_{2h} isomer, which are not involved in the central cavity, agree partly with their counterparts for the C_{4v} isomer. The two equivalent isoindole subunits (under D_{2h} symmetry) have bond lengths that closely agree with the bond lengths under C_{4v} symmetry, whereas the other two equivalent isoindole subunits have C−C bond lengths about 2 pm longer than the corresponding bond lengths for the C_{4v} structure. Despite several attempts, it was not possible to repeat the results using B3LYP/cc-pVTZ/cc-pVTZ-PP(Sn) due to convergence problems.

The structural parameters for C_{4v} symmetry obtained at the B3LYP/6-311++G**/cc-pVTZ-PP(Sn) and the B3LYP/cc-pVTZ/cc-pVTZ-PP(Sn) theory levels are in good agreement with each other and in good agreement with the B3LYP/DZVP computed counterparts (Table 2). However, the B3LYP/LANL2DZdp calculation predicts bond lengths which are shorter, especially the N−Sn bond length and the height of the Sn atom above the plane formed by the isoindole N atoms. We thought that this difference could be related to the fact that diffuse functions are included in the LANL2DZdp basis set. Therefore, we performed a B3LYP/6-311++G**/aug-cc-pVTZ-PP(Sn) calculation; however, the structure parameters obtained

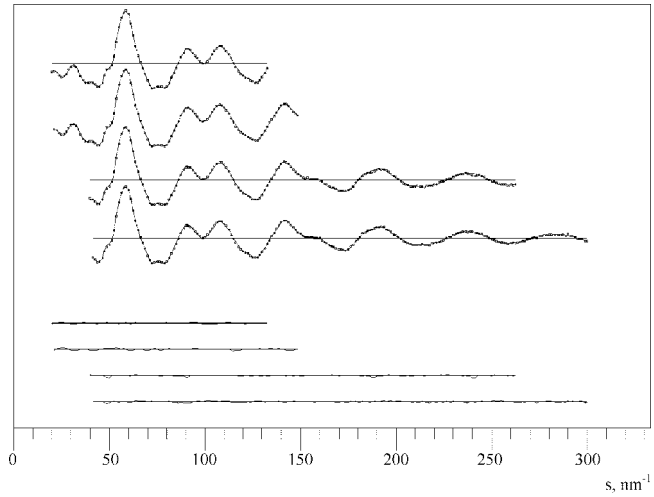

Figure 2. Average molecular intensity curves for Sn(II)Pc. The first two curves are the averages from eight sectors from the long camera distance along the *y*- and *x*-axis, respectively. The two next curves are the corresponding average curves from eight sectors from the middle camera distance. Dots are experimental points, and the full line is the theoretical curve. The four curves below are difference curves.

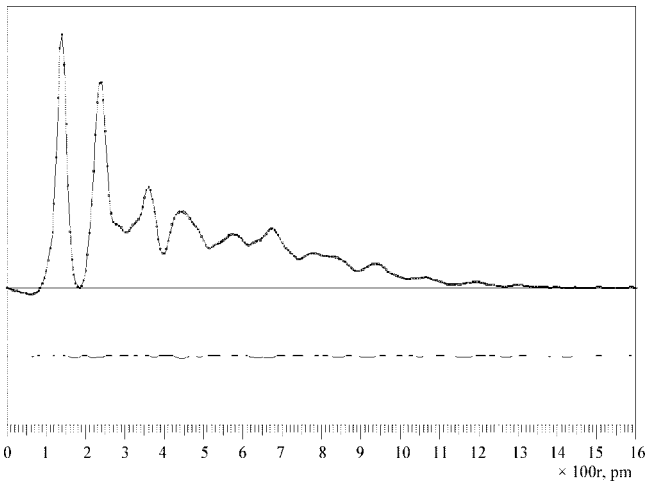

Figure 3. Radial distribution (RD) curves for Sn(II)Pc. The experimental points (dots) are the average of the four curves shown in Figure 2, and theoretical points are used for the unobserved region $s < 20.00$ nm^{-1}. The damping coefficient for the RD function is 35 pm^2. The curve below is the difference curve.

in this calculation were very close to the B3LYP/6-311++G**/cc-pVTZ-PP(Sn) calculation. This suggests that the differences are not related to diffuse functions. The Cartesian coordinates for the B3LYP/cc-pVTZ/cc-pVTZ-PP(Sn) are given as Supporting Information.

The B3LYP/6-311++G**/cc-pVTZ-PP(Sn) predicts five low normal mode frequencies. They are 18 cm^{-1} (B_1), where the two opposed isoindole fragments are moving up and the other two down, 33 cm^{-1} (A_1), which is a breathing motion where the four isoindole subunits are moving up and down, two frequencies of value 53 cm^{-1} (E), where the two opposite isoindole fragments are moving up or down and the two others are twisting, and 54 cm^{-1} (B_2), associated with the propeller twisting of the isoindole subunits.

Experimental Structure. The experimentally derived GED structure parameters together with their theoretically computed values, X-ray values, and previous GED structure parameters are presented in Table 4. The comparison of the X-ray structure with the calculated equilibrium structure is not straightforward because of different symmetries. However, the parameters agree rather well, with the exception of the N1−Sn57 bond length. This fact indicates that the crystal packing forces have no strong influence on the structure of the Pc macrocycle and that the position of the center of the electron density around the atoms and the position of the nuclei coincide.

The r_a parameter from GED represents an average over all vibrational level where each level is populated according to the Boltzmann distribution law. Usually, if there are no low vibrational modes, the estimated $r_e - r_a$ differences from the SHRINK program give a good estimation of the r_e structure. However, in this case, there are four different vibrational frequencies below 55 cm^{-1}, and all of them are related to out-of-plan motions. The notation $r_{e(ave)}$ is used for the estimated GED equilibrium structure given in Table 4 to emphasize the inherent difference between the GED $r_{e(ave)}$ structure and the quantum chemical r_e structure. It is the structure parameters related to the planarity of the macrocycle that are mostly influenced by the low vibrational modes, and this is clearly shown in Table 4.

The same tendency as that for the X-ray structure can be observed comparing the GED $r_{e(ave)}$ structure and the B3LYP equilibrium structure. There is good agreement for the C−N and the C−C bond lengths; however, disagreement can be seen for the N1−Sn57 and the C−H bond lengths. The C−H bond lengths cannot be accurately determined by GED due to the low scattering power of the H atoms. The GED $r_{e(ave)}$(N1−Sn57) = 226.0(10) pm is in very good agreement with corresponding X-ray values of 225.3 and 226.7 pm. The difference between the DFT-calculated value and the GED value is 3.4 pm, and this is larger than the estimated error limits for the GED parameter. A similar trend has been found for small organometallic tin molecules such as vinylstannane ($H_2C{=}CHSnH_3$),[39] allylstannane ($H_2C{=}CHCH_2SnH_3$),[38] and allenylstannane ($H_2C{=}C{=}CHSnH_3$),[38] where the Sn atom is attached to a π-conjugated system of carbon atoms. The B3LYP calculation using the same basis sets overestimated the C−Sn bond lengths compared to those of the GED r_e structure. These overestimations are 0.5 pm for vinylstannane, 1.7 pm for allylstannane, and 2.6 pm for allenylstannane.

Some of the GED bending angles differ from their B3LYP-calculated counterparts. Good agreements were found for the A1−N1−Sn57 = a1 and A2−N1−Sn57 = a2 + 90° angles, which define the position of the Sn atom above the plane of the four isoindole N atoms, and the pyramidality of the isoindole N atom.

Differences between GED and DFT for the N1−A2−A3 = a3 + 90° and the A2−A3−A4 = a4 + 90° angles associated with envelope bending of the pyrrole ring and the bending about the C13−C14 bond are found. These differences can be related to the presence of the low frequencies which perform waving and twisting motion of the isoindole subunits. The curvilinear treatment of vibrating atoms is the best available approximation at the moment, but it seems as if it is not good enough for a proper description of the flexible isoindole subunits. It is important to notice that there is a strong correlation between the a2 and the a3 refined angles (correlation coefficient = −0.88).

The A6−A7−N56 angle is about 5.5° smaller than the B3LYP-computed value. This is a significant difference. However, the refinement of this angle was tested many times using different variation schemes, and a value of about 80° was obtained for all schemes, and this is certainly an effect of the low-frequency modes. There is no strong correlation between the A6−A7−N56 angle and other parameters.

The agreement between the previous and our present GED study is not quite as good as expected. The $r_e - r_a$ corrections calculated by the SHRINK program and listed in Table 4 show that the r_e bond lengths must be shorter than the corresponding r -parameters. Therefore, the N1−Sn57 bond length of r_a value 220.1 pm in previous GED study has an r_e distance of 218.5 pm, which is much shorter than the N1−Sn57 bond length (226.0(10) pm) obtained in our study. The geometrical parameters regarding the Pc macrocycle agree within error limits, which are unusually large. The structural parameters obtained in this work and the structural parameters determined by X-ray and calculated by the DFT method are, generally, in much better agreement than those in the previous GED investigation.

The importance of including shrinkage corrections for the structure determination of Pc complexes has been outlined previously for HPc-Zn(II) and FPc-Zn(II).[12] Shrinkage corrections are used in the present reinvestigation; a larger data range increases the precision, reliability, and accuracy of the structure parameters of Sn(II)Pc, making comparison between structure parameters obtained from GED, X-ray, and DFT meaningful and raising the question about the comparability of the structure

parameters from these three different methods, which all together justify this reinvestigation of Sn(II)Pc.

Acknowledgment. The University of Oslo is thanked for a generous amount of computer time. S. Gundersen is acknowledged for workup of the experimental data. T.S. thanks the International Student Quota Program of the University of Oslo for financial support.

Supporting Information Available: Cartesian coordinates for B3LYP/cc-pVTZ/cc-pVTZ-PP(Sn) and C_{4v} symmetry (Table S1) and vibrational frequencies and IR intensities for B3LYP/6-311++G**/cc-pVTZ-PP(Sn) and C_{4v} symmetry (Table S2). This material is available free of charge via the Internet at http://pubs.acs.org.

References and Notes

(1) Forrest, S. R. *Chem. Rev.* **1997**, *97*, 1793.
(2) Imanishi, Y.; Ishihara, S.; Hamada, T. *Mol. Cryst. Liq. Cryst. Sci. Technol., Sect. A* **1998**, *315*, 413.
(3) Imanishi, Y.; Ishihara, S. *Thin Solid Films* **1998**, *331*, 309.
(4) Dirk, C. W.; Inabe, T.; Schoch, K. F., Jr.; Marks, T. J. *J. Am. Chem. Soc.* **1983**, *105*, 1539.
(5) Papageorgiou, N.; Salomon, E.; Angot, T.; Layet, J.-M.; Giovanelli, L.; Le Lay, G. *Prog. Surf. Sci.* **2005**, *77*, 139.
(6) Beltran, H. I.; Esquivel, R.; Lozada-Cassou, M.; Dominguez-Aguilar, M. A.; Sosa-Sanchez, A.; Sosa-Sanchez, J. L.; Hoepfl, H.; Barba, V.; Luna-Garcia, R.; Farfan, N.; Zamudio-Rivera, L. S. *Chem.— Eur. J.* **2005**, *11*, 2705.
(7) Walzer, K.; Hietschold, M. *Surf. Sci.* **2001**, *471*, 1.
(8) Arnold, D. P.; Blok, J. *Coord. Chem. Rev.* **2004**, *248*, 299.
(9) Shannon, R. D.; Prewitt, C. T. *Acta Crystallogr., Sect. B* **1969**, *25*, 925.
(10) Fischer, M. S.; Weiss, C., Jr. *J. Chem. Phys.* **1970**, *53*, 3121.
(11) Whitten, D. G.; Yau, J. C. N.; Carroll, F. A. *J. Am. Chem. Soc.* **1971**, *93*, 2291.
(12) Strenalyuk, T.; Samdal, S.; Volden, H. V. *J. Phys. Chem. A* **2007**, *111*, 12011.
(13) Engel, M. K. *Kawamura Rikagaku Kenkyusho Hokoku* **1997**, 11.
(14) Friedel, M. K.; Hoskins, B. F.; Martin, R. L.; Mason, S. A. *J. Chem. Soc. D* **1970**, 400.
(15) Kubiak, R.; Janczak, J. *J. Alloys Compd.* **1992**, *189*, 107.
(16) Bennett, W. E.; Broberg, D. E.; Baenziger, N. C. *Inorg. Chem.* **1973**, *12*, 930.
(17) Janczak, J.; Kubiak, R. *J. Alloys Compd.* **1994**, *204*, 5.
(18) Hulme, R. *J. Chem. Soc.* **1963**, 1524.
(19) Day, P. N.; Wang, Z.; Pachter, R. *THEOCHEM* **1998**, *455*, 33.
(20) Zhang, Y.; Zhang, X.; Liu, Z.; Xu, H.; Jiang, J. *Vib. Spectrosc.* **2006**, *40*, 289.
(21) Ruan, C.-y.; Mastryukov, V.; Fink, M. *J. Chem. Phys.* **1999**, *111*, 3035.
(22) Samdal, S.; Volden, H. V.; Ferro, V. R.; Garcia de la Vega, J. M.; Gonzalez-Rodriguez, D.; Torres, T. *J. Phys. Chem.* **2007**, *111*, 4542.
(23) Zeil, W.; Haase, J.; Wegmann, L. *Z. Instrumentenkd.* **1966**, *74*, 84.
(24) Gundersen, S.; Samdal, Svein, Strand, Tor, G.; Volden, Hans, V. *J. Mol. Struct.* **2007**, *832*, 164.
(25) Gundersen, S.; Samdal, S.; Seip, R.; Strand, T. G. *J. Mol. Struct.* **2004**, *691*, 149.
(26) Frisch, M. J.; Trucks, G. W.; Schlegel, H. B.; Scuseria, G. E.; Robb, M. A.; Cheeseman, J. R.; Montgomery, J. A., Jr.; Vreven, T.; Kudin, K. N.; Burant, J. C.; Millam, J. M.; Iyengar, S. S.; Tomasi, J.; Barone, V.; Mennucci, B.; Cossi, M.; Scalmani, G.; Rega, N.; Petersson, G. A.; Nakatsuji, H.; Hada, M.; Ehara, M.; Toyota, K.; Fukuda, R.; Hasegawa, J.; Ishida, M.; Nakajima, T.; Honda, Y.; Kitao, O.; Nakai, H.; Klene, M.; Li, X.; Knox, J. E.; Hratchian, H. P.; Cross, J. B.; Adamo, C.; Jaramillo, J.; Gomperts, R.; Stratmann, R. E.; Yazyev, O.; Austin, A. J.; Cammi, R.; Pomelli, C.; Ochterski, J. W.; Ayala, P. Y.; Morokuma, K.; Voth, G. A.; Salvador, P.; Dannenberg, J. J.; Zakrzewski, V. G.; Dapprich, S.; Daniels, A. D.; Strain, M. C.; Farkas, O.; Malick, D. K.; Rabuck, A. D.; Raghavachari, K.; Foresman, J. B.; Ortiz, J. V.; Cui, Q.; Baboul, A. G.; Clifford, S.; Cioslowski, J.; Stefanov, B. B.; Liu, G.; Liashenko, A.; Piskorz, P.; Komaromi, I.; Martin, R. L.; Fox, D. J.; Keith, T.; Al-Laham, M. A.; Peng, C. Y.; Nanayakkara, A.; Challacombe, M.; Gill, P. M. W.; Johnson, B.; Chen, W.; Wong, M. W.; Gonzalez, C.; Pople, J. A. *Gaussian 03*, revision B.03; Gaussian, Inc.: Pittsburgh, PA, 2003.
(27) Becke, A. D. *J. Chem. Phys.* **1993**, *98*, 5648.
(28) Lee, C.; Yang, W.; Parr, R. G. *Phys. Rev. B* **1988**, *37*, 785.
(29) Godbout, N.; Salahub, D. R.; Andzelm, J.; Wimmer, E. *Can. J. Chem.* **1992**, *70*, 560.
(30) Andzelm, J.; Wimmer, E. *J. Chem. Phys.* **1992**, *96*, 1280.
(31) Wadt, W. R.; Hay, P. J. *J. Chem. Phys.* **1985**, *82*, 284.
(32) Check, C. E.; Faust, T. O.; Bailey, J. M.; Wright, B. J.; Gilbert, T. M.; Sunderlin, L. S. *J. Phys. Chem. A* **2001**, *105*, 8111.
(33) Krishnan, R.; Binkley, J. S.; Seeger, R.; Pople, J. A. *J. Chem. Phys.* **1980**, *72*, 650.
(34) Frisch, M. J.; Pople, J. A.; Binkley, J. S. *J. Chem. Phys.* **1984**, *80*, 3265.
(35) Peterson, K. A. *J. Chem. Phys.* **2003**, *119*, 11099.
(36) Metz, B.; Stoll, H.; Dolg, M. *J. Chem. Phys.* **2000**, *113*, 2563.
(37) Dunning, T. H., Jr. *J. Chem. Phys.* **1989**, *90*, 1007.
(38) Strenalyuk, T.; Samdal, S.; Mollendal, H.; Guillemin, J.-C. *Organometallics* **2006**, *25*, 2090.
(39) Strenalyuk, T.; Samdal, S.; Mollendal, H.; Guillemin, J.-C. *Organometallics* **2006**, *25*, 2626.
(40) Sipachev, V. A. *J. Mol. Struct.: THEOCHEM* **1985**, *22*, 143.
(41) Sipachev, V. A. *J. Mol. Struct.* **2001**, *567−568*, 67.
(42) Gundersen, G.; Samdal, S.; Seip, H.-M.; Strand, T. G. *Annual Report from the Norwegian Gas Electron Diffraction Group*; **1977, 1980, 1981**.
(43) Liao, M.-S.; Scheiner, S. *Mol. Phys.* **2003**, *101*, 1227.
(44) Ruan, C.-y.; Mastryukov, V.; Fink, M. *J. Chem. Phys.* **1999**, *111*, 3035.

JP804809E